Projections and uncertainties of future winter windstorm damage in Europe

Luca G. Severino[1], Chahan M. Kropf[2,3], Hilla Afargan-Gerstman[1], Christopher Fairless[2], Andries Jan de Vries[4], Daniela I.V. Domeisen[4,1], and David N. Bresch[2,3]

[1]Institute for Atmospheric and Climate Science, ETH Zürich, Zürich, Switzerland
[2]Institute for Environmental Decisions, ETH Zürich, Zürich, Switzerland
[3]Federal Office of Meteorology and Climatology MeteoSwiss, Zürich, Switzerland
[4]Institute of Earth Surface Dynamics, University of Lausanne, Lausanne, Switzerland

Correspondence: Luca Severino (luca.severino@usys.ethz.ch)

Abstract.

Winter windstorms are among the most significant natural hazards in Europe linked to fatalities and substantial economic damages. However, projections of windstorm impact in Europe under climate change are highly uncertain. This study combines climate projections from 30 general circulation models participating in CMIP6 with the climate-risk assessment model CLIMADA to obtain projections of future change in windstorm-induced damages over Europe. We conduct an uncertainty-

5   sensitivity analysis, and find large uncertainties in the projected changes in the damages, with climate model uncertainty being the dominant factor of uncertainty in the projections. We investigate spatial patterns of the future changes in windstorm damages and find an increase in the damages in northwestern and northern-central Europe, and a decrease over the rest of Europe, in agreement with an eastward extension of the North Atlantic storm track into Europe. We combine all 30 available climate

10   models in an ensemble of opportunity approach and find evidence for an intensification of future windstorm damages, with damages with return periods of 100 years under current climate conditions becoming damages with return periods of 28 years under future SSP585 climate scenarios. Our findings demonstrate the importance of climate model uncertainty for the CMIP6 projections of windstorms in Europe, and emphasize the increasing need for risk mitigation due to extreme weather in the future.

15   **1   Introduction**

Extratropical cyclones (ETCs) can cause intense windstorms in winter (hereafter referred to as *winter storms*), and are among the most significant natural hazards in Europe in terms of fatalities and damages to physical assets (Schwierz et al., 2010). Understanding future changes in winter storm risk is thus key for risk assessment and damage mitigation in Europe.

Both the main regions of extratropical cyclonic activity (known as the storm tracks) and the characteristics of individual

20   ETCs are expected to change as climate changes (Shaw et al., 2016; Catto et al., 2019). Many studies suggest an eastward extension of the North Atlantic storm track further into Europe, potentially increasing the risk of winter storms and their regional impacts (Zappa et al., 2013; Zappa and Shepherd, 2017; Oudar et al., 2020; Harvey et al., 2020; Priestley and Catto,

2022). However, changes in the North Atlantic storm track are highly uncertain, as climate models feature biases in both the location and the dynamical intensity of the storm tracks (Lee et al., 2021). For instance, General Circulation Models (GCMs)

25 participating in the Coupled Model Intercomparison Project (CMIP) are associated with a winter storm track extending too zonally into Europe (Harvey et al., 2020; Priestley et al., 2020), and tend to underestimate the intensity of the most intense ETCs (Seiler and Zwiers, 2016; Priestley et al., 2020). In addition, the level of global warming will likely be an important factor of uncertainty, with emission scenarios corresponding to higher radiative forcings potentially further increasing both the number and the intensity of ETCs associated with strong wind speeds over northwestern Europe (Zappa et al., 2013).

Modelling the impacts of winter storms and their strong winds can be achieved by incorporating surface wind projections from climate models into climate-risk models, thus using the risk framework to derive estimates of natural hazard-related impacts on natural or socio-economic systems. In the risk framework, risk from a natural hazard can be modelled as the convolution between three components: the hazard, the exposure, and the vulnerability (IPCC, 2014). The hazard describes the

35 distribution of the intensity of a certain hazard in space and time (e.g. wind gust intensities, flooding heights), the exposure describes the distribution of assets at risk in space and time (e.g. population, infrastructure, crops, ecosystems), and the vulnerability makes the link between hazard and exposure, by describing the effect of the hazard on the exposed value in terms of the assessed impact. Most often, the complex hazard-exposure-impact relation of the vulnerability component is approximated with simpler functional relationships, called *vulnerability curves*, or *impact functions*.

40 By incorporating the three components of risk, climate-risk models can jointly assess changes in exposure and vulnerability and changes in the climate system, thus allowing to produce comprehensive estimates of climate impacts. These estimates of climate impacts are extremely valuable for the mitigation and management of changing climate risks, and can greatly help to improve the resilience of our societies or of the natural environment to climate change.

45 Considerable uncertainties are involved in the modelling of the hazard, exposure and vulnerability, which in turn can contribute to render risk projections highly uncertain. Understanding and quantifying those uncertainties, and their influence on the outcome of the risk projection is crucial for risk assessment studies. Uncertainty and sensitivity analyses are a commonly used method to study and model uncertainties associated with the use of complex models such as climate-risk models (Saltelli et al., 2008; Pianosi et al., 2016; Kropf et al., 2022). Uncertainty and sensitivity analyses rely on the generation of many replications

50 of a model's output, where the replications are obtained by varying some of the model's input factors which are considered as uncertain. The term *input factors* here refers to any of the model's components (e.g. parameters, data) which can drive a variation in any of the model's outputs, while the term *outputs* refers to any numerical results produced by the model (Saltelli et al., 2008, 2019). Uncertainty analysis can then be understood as the study of the distribution of the generated model outputs, and sensitivity analysis as the study of the links between the model's uncertain input factors and the generated model outputs.

55 Uncertainty and sensitivity analyses can thus provide insights into which of the model's input factors contribute most to the uncertainty in model output, and help in understanding the model's input-output relationships.

Many studies have focused on past (e.g. Della-Marta et al., 2010; Donat et al., 2010b; Haylock, 2011; Priestley et al., 2018; Vautard et al., 2019; Walz and Leckebusch, 2019; Koks and Haer, 2020; Welker et al., 2021; Röösli et al., 2021; Wilkinson
60   et al., 2022) or future (e.g. Leckebusch et al., 2007; Heneka et al., 2007; Pinto et al., 2007; Schwierz et al., 2010; Donat et al., 2011; Pinto et al., 2012; Ranson et al., 2014; Karremann et al., 2014; Hochman et al., 2022) impacts of extratropical winter windstorms in Europe. For instance, Pinto et al. (2007) assessed future European winter storm damages considering multiple realizations of a single climate model with varying initial conditions and boundary forcing scenarios, and Leckebusch et al. (2007) and Donat et al. (2011) assessed future European winter storm damages considering different climate models.
65   However, no attempt has been made to use the most recent projections from climate models participating in phase six of the Coupled Model Intercomparison Project (CMIP6; Eyring et al., 2016) to conduct a multi-model and multi-scenario assessment of winter storm related wind damages in Europe. Furthermore, a few uncertainty and sensitivity analyses focusing on winter storm damage risk modelling under current climate have been published (e.g. Koks and Haer, 2020; Röösli et al., 2021), but a comprehensive estimate of the importance of the different uncertainties involved in the modelling of winter storm damage in
70   Europe under future climate is still lacking.

This study combines state-of-the-art climatic projections from 30 global climate models participating in CMIP6 with the open-source weather and climate risk assessment model CLIMADA to obtain a set of relevant projections for future winter-storm-induced wind damages over Europe. CLIMADA's uncertainty-sensitivity quantification module *unsequa* (Kropf et al.,
75   2022) is used to quantify the importance of five different sources of uncertainty in the projections: Climate model, internal climate variability, future climate scenario, exposure, and impact function uncertainty.

This paper is structured as follows: Sect. 2 introduces hazard, exposure, and vulnerability data, and presents the damage and uncertainty modelling approaches; Sect. 3 presents the results of both the uncertainty and sensitivity quantification, and the
80   future winter storm damage projections; Sect. 4 summarizes, discusses the results, and concludes.

2   Data and methods

This study uses the open-source weather and climate risk modelling platform CLIMADA (Aznar-Siguan and Bresch, 2019) to estimate windstorm damages associated with European winter storms in a changing climate. The term damage here represents the economic losses resulting from the impact of intense surface wind gusts on physical assets. CLIMADA is based on the risk
85   framework as defined by the IPCC (IPCC, 2014) that incorporates the three components hazard, exposure, and vulnerability to compute impact and risk metrics in a fully probabilistic and geographically explicit manner. Additionally, CLIMADA features an uncertainty and sensitivity quantification module (*unsequa*; Kropf et al., 2022), which is used in this study to assess the key uncertainties associated with the modelling of the damages. See Fig. 1 for a visual summary of the study framework. We study the impact of climate change on winter storm damage over Europe, by combining hazard data modelled for a domain
90   comprised within latitudes 30° to 75°N and longitudes 30°W to 30°E with exposure data for 44 European countries. To better

explore the spatial patterns of the damages, specific countries are grouped into seven sub-regions shown in Fig. 2, the British Isles (BI), the Iberian Peninsula (IP), Western Europe (WEU), Central Europe (CEU), the Mediterranean and Balkan region (MED), Scandinavia (SC), and Eastern Europe (EEU). The seven sub-regions are defined following their climate and their exposure to winter storm hazards, following Christensen and Christensen (2007). Damages are investigated on a daily basis,

95 for the winter half-year only (October-November-December-January-February-March). Climate change effects are studied by comparing damages computed for a future (2070-2100) versus a historical (1980-2010) period. GCMs participating in CMIP6 are used to represent past and future climates and their surface winds as described in Sect. 2.1. Exposure and vulnerability data are described in Sect. 2.2 and 2.3. Section 2.4 describes the different damage and risk metrics used in this study, and Sect. 2.5 briefly details the methods and results of the model's calibration and validation procedures. Finally, Sect. 2.6 introduces the

100 *unsequa* module and explains the uncertainty and sensitivity quantification framework.

2.1 CMIP6 windstorm hazard data

We use daily surface wind maximum (sfcWindmax) outputs from 30 GCMs participating in CMIP6 to represent winter storm hazards. Model data is kept on the original model grids, as provided by the modelling centers. We select the GCMs on the criterion that a GCM provides at least one simulation for the historical period and one simulation for the future period, obtained

105 using the forcing dataset from the Shared Socio-economic Pathway 5-8.5 (hereafter SSP585; for a detailed description of the shared socio-economic pathways and CMIP6 scenarioMIP experiments, see O'Neill et al., 2016). We choose the high-emission SSP585 scenario as we expect it to correspond to a high-impact scenario (Zappa et al., 2013). For each GCM, a maximum of three ensemble members is considered. One ensemble member of the historical and one ensemble member of the SSP585 simulations from the GCM NESM3 were discarded from the analysis due to a strong negative bias in the surface wind speeds

110 of the historical member, which resulted in a strong positive bias in future-minus-historical change in surface wind maxima. Table A1 summarizes the climate models and climate model members used for the damage projections of this study. Model members representing the same GCM-SSP combination are assembled into one single simulation in order to decrease the effects of internal variability. Thus, for each of the study periods (historical or future), we obtain hazard data with a duration of 30, 60, or 90 years, for climate models with respectively one, two, or three ensemble members. First, we consider each

115 climate model separately to compute the damage projections (Sect. 3.2). Considering the climate models separately allows us to investigate the climate model uncertainty in the projections. As a second step, we combine the different climate models, in an ensemble of opportunity approach (Tebaldi and Knutti, 2007), where all models are considered to be equally valid realizations of the climate and combined without prior weighting (Sect. 3.3). This ensemble of opportunity approach allows us to consider simulations representing 600 winter seasons, which can be used to estimate damage events with considerably longer return

120 periods.

We use a percentile mapping technique originally designed in Rajczak et al. (2016) and adapted by Lüthi et al. (2022) to bias-correct the GCMs' daily sfcWindmax outputs. ERA5 10m wind gust maxima (WG10) are used as reference for the bias correction. Hourly WG10 data are first resampled to a daily resolution and then linearly interpolated to each CMIP6 GCM's grid. A bias-correction is then carried out for each climate model's grid-cell, using one single correction function per GCM,
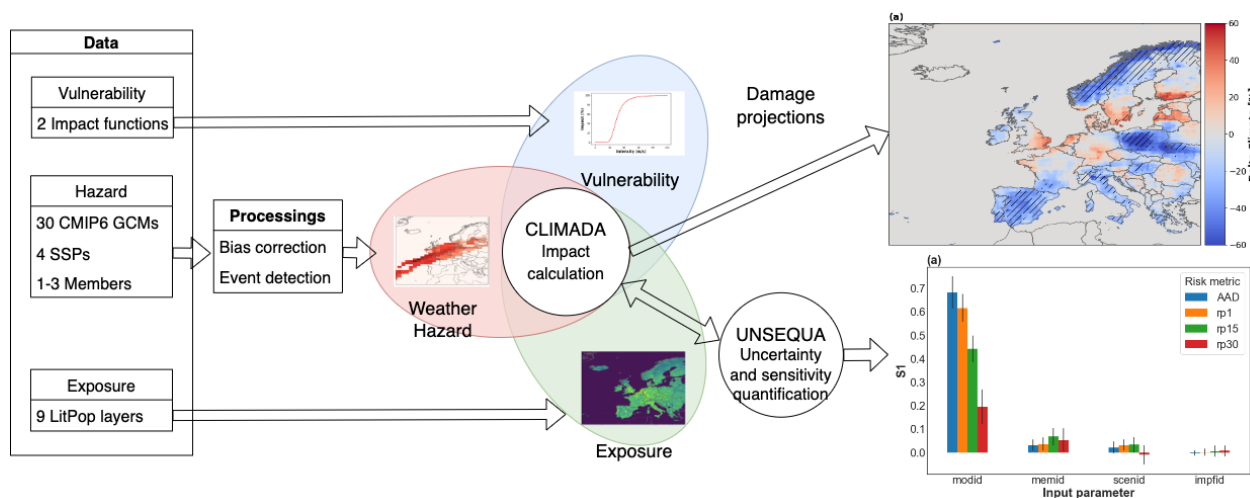
Figure 1. Schematic describing the modelling process. Thirty General Circulation Models (GCMs) participating in phase six of the Coupled Model Intercomparison Project (CMIP6) and featuring one to three ensemble members are used to represent the winter climate from a historical (1980-2010), and a future (2070-2100) period, resulting in 67 members x 30 years x 6 months = 12060 months of winter climate for each period. The historical climates are obtained from CMIP6's historical experiments and the future climates from the Shared Socioeconomic Pathway 5-8.5 (SSP585) experiments. Daily surface wind maximum outputs from each GCM are bias-corrected using a percentile mapping approach, and storm days are detected from the pre-processed daily surface wind maximum fields from those 2 x 12060 months of winter climate. The storm days derived from the GCMs, exposure data from the Litpop dataset, and a storm damage impact function taken from Schwierz et al. (2010) are then incorporated as the weather hazard, exposure, and vulnerability data into the weather and climate risk assessment model CLIMADA, which then produces damages and risk metrics, such as damage maps, or Exceedance-Frequency-Curves. We use those damage and risk metrics to obtain *delta climate* estimates, where *delta climate* refers to the future-minus-historical change in the metric relative to the historical period. As a second step, CLIMADA's uncertainty and sensitivity quantification module (*unsequa*) is used to study the uncertainty and sensitivity related to the hazard, exposure, and vulnerability components in the damage projections. To this end, we generate additional hazard data from 14 GCMs featuring three realizations for each of the historical, SSP126, SSP245, SSP370, and SSP585 experiments from CMIP6; eight additional exposure data layers using different parameterizations of LitPop; and an additional storm damage impact function taken from Klawa and Ulbrich (2003). This additional hazard, exposure, and vulnerability data is then used by CLIMADA's *unsequa* module to quantify the uncertainty in several damage and risk metrics, including the Average Annual Damage (AAD), and damage amounts with return periods, of one, 15, and 30 years (rp1, rp15, rp30), and to assess the sensitivity of those damage and risk metrics to different components of the modelling framework, including $modid$: climate model choice; $memid$: climate model member choice; $scenid$: future climate scenario choice; and $impfid$: impact function choice.

125 so that inter-member variability is preserved. For each climate model, the correction function is computed as the average correction function taken over the different ensemble members of the climate model.

We detect stormy days associated with European winter storms from the bias-corrected daily GCM data by applying a simple selection procedure, based on local wind statistics. A storm event is defined as a day for which stormy conditions are locally
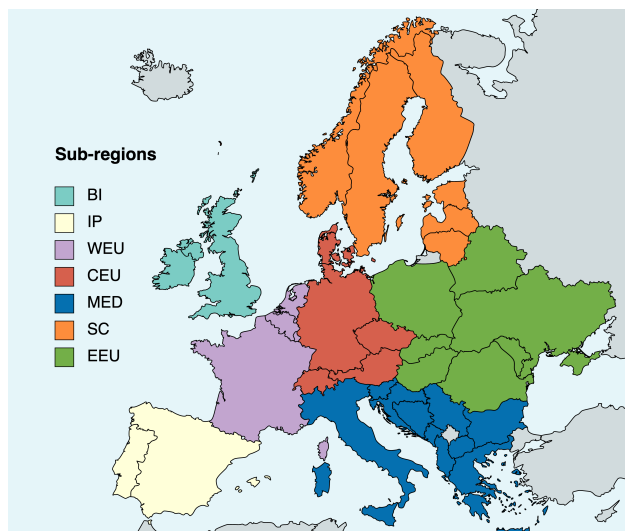
Figure 2. Map of the seven sub-regions used for regional winter storm damage assessment: the British Isles (BI; United Kingdom, Ireland), the Iberian Peninsula (IP; Spain, Portugal, Andorra), Western Europe (WEU; France, Monaco, Kingdom of the Netherlands, Luxembourg, Belgium), Central Europe (CEU; Switzerland, Germany, Liechtenstein, Czech Republic, Austria), the Mediterranean and Balkan region (MED; Italy, Albania, Bosnia and Herzegovina, Croatia , Montenegro , Malta, Greece, San Marino, Vatican City State, Slovenia, Macedonia, Bulgaria, Serbia), Scandinavia (SC; Denmark, Sweden, Finland, Norway, Estonia, Latvia, Lithuania), and Eastern Europe (EEU; Belarus, Hungary, Poland, Romania, Slovakia, Ukraine, Republic of Moldova). Physical asset exposure is modelled for each of the listed countries using the LitPop dataset (Sect. 2.2).

detected over a part of the domain. First, a grid-cell of a GCM's grid is considered as stormy if the daily intensity of the
130 sfcWindmax is in excess of its local 98th percentile value, computed over the winter half-years of the historical simulation of
the model. The choice of the 98th percentile value as a threshold has been widely used for winter storm damage assessment
studies (e.g., Klawa and Ulbrich, 2003; Pinto et al., 2007; Schwierz et al., 2010; Donat et al., 2010a, 2011), and is based on the
assumption that storms and associated damages only occur during the two percent windiest days of the winter half-year (Klawa
and Ulbrich, 2003). This modelling approach does not assume any temporal adaptation to future changes in the wind climate,
135 as the local wind speeds thresholds are constant in time and representative of the historical wind conditions only. We also
ensure that the selected daily wind fields correspond to wind intensities that are sufficiently intense to produce actual damages
by further requiring the daily wind intensities to be greater than a value of $15 \text{ m} \cdot \text{s}^{-1}$ to be considered as stormy (Schwierz
et al., 2010). Only grid-cells that fulfill both conditions are considered for the subsequent damage calculations. Secondly, the
total area of the stormy grid-cells on a particular day must amount to a minimum threshold A_{min} for the day to be considered
140 as stormy. A value of 15000 km^2 is chosen for A_{min}, which is representative of the typical area of the wind footprint of an
extratropical storm (Kruschke, 2014). Days that do not fulfill this minimum area requirement are not considered in the analysis,

thus noise and small-scale events unrelated to European winter storms are filtered out. In summary, a stormy day is defined as:

$$\text{Stormy day}_t \iff \sum_i \{a_i|[(v_{i,t} \geq v_{i,98}) \;\&\; (v_i \geq 15)]\} \geq A_{min} \tag{1}$$

where a_i is the area of the grid cell i, $v_{i,t}$ is the daily sfcWindmax intensity at grid cell i on the considered day t, $v_{i,98}$ is the

145 98th percentile of the daily sfcWindmax at grid cell i, computed over the winter periods of the historical period, and A_{min} is the area threshold parameter.

2.2 LitPop exposure data

We use the LitPop dataset to represent exposure (Eberenz et al., 2020). LitPop provides geographical distribution of physical asset exposure, by spatially disaggregating country-specific macroeconomic indicators (e.g. produced capital, growth domestic

150 product) using nightlight intensity and population count data. For this study we choose produced capital as the macroeconomic indicator, which we distribute in space at a resolution of 600 arcseconds and using the base parameterization of LitPop, which gives equal weight to the nightlight and population disaggregation layers. We assume no future change in population and economy, and thus keep the exposed values and their geographical distribution constant in time.

2.3 Vulnerability

155 CLIMADA uses impact functions to represent vulnerability. Those impact functions link input wind gusts intensity to a mean damage degree (MDD), representing the percentage of the exposure asset value damaged at the given wind intensity. Thus, each daily hazard value at each of the hazard data grid-cells is converted into a MDD, which CLIMADA then combines to the LitPop exposure data to compute damages at the exposure level. We only consider one single impact function for the entire domain and do not differentiate between the different asset types (e.g. residential, industrial). Considering only one single

160 impact function allows us to avoid a complex calibration procedure requiring the tuning of numerous parameters. We use primarily one impact function, which has been designed in Schwierz et al. (2010, hereafter Sw2010), and which is already implemented in CLIMADA. This function has been directly derived from an insurer's loss model and is based on past claim data in the United Kingdom and cross-validated with other European countries.

As a second step, we test the sensitivity of our results by considering a different impact function, which uses wind speed values

165 above a threshold instead of absolute wind intensity. This excess-over-threshold impact function (hereafter CubEOT) relies on the assumption that damages only occur when wind is in excess of a local threshold, computed at the grid-cell level, and that the damages are proportional to the cube of the excess-over-threshold intensity. This cubic excess-over-threshold relation has first been derived by Klawa and Ulbrich (2003), and then further used in a number of studies modelling winter storm damage in Europe (e.g., Pinto et al., 2007; Leckebusch et al., 2007; Donat et al., 2010b, 2011; Pinto et al., 2012). Consistent with our

170 event definition, we use as a local threshold value the 98th percentile of the daily surface wind maximum computed over the historical period. We also give an upper limit to the damages potentially achievable, by assuming a constant MDD when wind intensities are more than double their 98th percentile value. The function CubEOT is defined as:
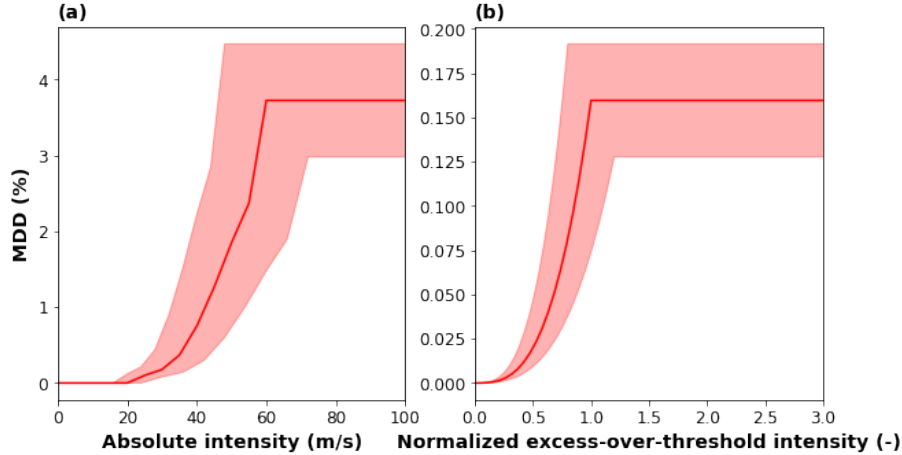
Figure 3. The two impact functions considered in this study. Panel (a) shows the empirical curve based on recorded winter storm losses from a reinsurance company from Schwierz et al. (2010); Panel (b) shows the Cubic excess-over-threshold from Klawa and Ulbrich (2003). For the two curves, the red bands indicate the calibration uncertainty accounted for in the uncertainty and sensitivity analysis (see Sect. 2.6).

$$
MDD_{i,t} = \begin{cases} MDD_{max} & \text{if } v_{i,t} > 2 \cdot v_{98,i} \\ MDD_{max} \cdot \left(\frac{v_{i,t}}{v_{98,i}} - 1 \right)^3 & \text{if } 2 \cdot v_{98,i} \geq v_{i,t} \geq v_{98,i} \\ 0 & \text{otherwise} \end{cases} \tag{2}
$$

where $MDD_{i,t}$ is the MDD computed for the day t and model grid cell i, MDD_{max} is a constant corresponding to the
maximum MDD achievable and determined during calibration, $v_{i,t}$ is the daily sfcWindmax for day t at model grid cell i, and
$v_{98,i}$ is the 98th percentile of the sfcWindmax variable at model grid cell i, computed over the winter periods of the historical
period. The Sw2010 and CubEOT impact functions are shown in Fig. 3.

2.4 Damage and risk metrics

We use primarily the following damage and risk metrics to present our damage projections:

1. *Average Annual Damage (AAD)*: The AAD represents the sum of all the damages occurring during a period, divided by
   the number of years in this period. The AAD is a relevant risk metric for the insurance industry, as it informs on the
   damages accumulated over a certain period.

2. *Exceedance Frequency Curves (EFCs)*: EFCs allow us to visualize the distribution of the damages in the frequency-
   intensity domain. Considering a damage event set covering a period of N years, we can order the damage events by
   intensity, and assign to each damage event an exceedance frequency. For instance, the intensity of the most intense

damage event being reached or exceeded only once over the whole period covered by the dataset, receives an exceedance frequency of $\frac{1}{N}$, and the intensity of the second most intense damage event reached or exceeded twice, receives an exceedance frequency of $\frac{2}{N}$, etc. Alternatively, one can consider the *Return Period (RP)* of an event, which is the inverse of the exceedance frequency, and corresponds to the time interval during which a certain event intensity is expected to
190 not be exceeded. It has to be noted that the intensity of an event with a certain return period is based on fewer events as the return periods considered increase, thus increasing the sampling uncertainty of the statistic (Welker et al., 2021). For instance, the intensity of an event with a return period of 30 years will be based on one event only for a 30-years-long dataset, and the intensity of a 15 years return period event will be based on two events.

This study investigates the changes in damages in both the spatial, and frequency-intensity dimension. Changes in the damages
195 in the spatial dimension are investigated using spatial maps of the change in the AAD, and by examining the inter-model distribution of the changes in AAD, and damage amounts with return periods of one and 15 years (rp1, rp15), aggregated to a regional level. Future changes in the AAD, rp1 and rp15 are presented in the form of a future-minus-historical change relative to the historical reference period, which we refer to as *delta climate*. For the computation of the spatial maps resolved at the exposure level, a constant value of one is added to the historical damages, to avoid dividing by zero in regions where
200 no damages are modelled during the historical period. Future changes of the damages in frequency-intensity dimension are investigated by comparing future vs historical EFCs of the damages aggregated to the entire study domain.

2.5   Model calibration and validation

We use WG10 from the ERA5 reanalysis regridded at $1° \times 1°$ resolution as hazard data to compute damages over a control period. We then compare the modelled damages to recorded damages retrieved from the EM-DAT database (Guha-Sapir, 2021).
205 The damages recorded in the EM-DAT database only cover a period spanning from 1998 to 2020, and we thus use the 12 years which overlap with our historical period of 1980 to 2010 as a control period. We first ensured that the AADs computed using each impact function over the control period reproduce to a reasonable order of magnitude the AAD computed with the recorded damages of EM-DAT. The Sw2010 impact function yielded realistic damage estimates but the CubEOT impact function required calibration, as it yields damage estimates that are higher by about two orders of magnitude in comparison to
210 the AAD of EM-DAT. We thus recalibrated the CubEOT impact function by rescaling its MDD scale by a multiplicative factor MDD_{max}, computed as the ratio of the AAD from EM-DAT over the ADD obtained with the uncalibrated CubEOT function during the control period:

$$MDD_{max} = \frac{AAD_{EM\text{-}DAT}}{AAD_{ERA5,control}} \tag{3}$$

Next, we controlled that both impact functions are able to produce realistic damage estimates for the ten storm events present
215 in the EM-DAT dataset (Anatol, Calvann, Cilly, Desiree, Fanny, Emma, Erwin, Jeanett, Klaus, Kyrill, Lothar, Martin; Cilly, Desiree, and Fanny are registered as a single storm event in the EM-DAT database). For all storm events, our modelling framework underestimates the damages, resulting in a mean absolute percentage error of 78% and 66% for the Sw2010 and CubEOT impact functions respectively. However, we consider those errors as acceptable in the scope of this study, and validate

our modelling framework, as it is able to produce sufficiently realistic damage estimates for major European winter storm
220 events.

2.6 Uncertainty and sensitivity quantification

The uncertainty and sensitivity analysis carried out in this study is done entirely with CLIMADA's *unsequa* module and
follows the essential steps described in Kropf et al. (2022). We first define input variables and input parameters that represent
relevant factors of uncertainty in the modelling of future winter storm damage over Europe. Those factors of uncertainty relate
225 to uncertainties in the modelling of the hazard, exposure, and vulnerability. We assess the uncertainty in the hazard data by
varying the GCMs and SSPs used to generate the storm days. In addition, we assess the effect of internal variability on the
hazard by considering different model members for each GCM-SSP combination. We thus select 14 GCMs that provide at least
three model members for the five experiments: *historical*, *SSP126*, *SSP245*, *SSP370*, and *SSP585*. The choice of the climate
model, future climate scenario, and model members are reflected by the $modid$, $scenid$, and $memid$ uncertainty parameters.
230 Each parameter is an integer index corresponding to a unique climate model, future climate scenrio, or model member, and
is drawn uniformly over the possible set of values for each uncertainty factor: $modid \in (0, 1, 2, ..., 13)$, $scenid \in (0, 1, 2, 3)$,
and $memid \in (0, 1, 2)$. We choose uniform distributions as we assume each of the possible parameter values to have equal
probability. Uncertainty in the modelling of the exposure is accounted for by varying the m and n exponents of the LitPop
exposure data, which respectively govern the weight given to the population count and nightlight intensity data layers used for
235 the spatial disaggregation. Varying the m and n exponents allows us to simulate uncertainty in the geographical distribution of
the physical assets, with higher values of n emphasizing highly populated areas, and lower values of n less densely populated
areas (Kropf et al., 2022). According to Eberenz et al. (2020), $m = 1$, and $n = 1$ is the best performing parameterization for
total value distribution in space. Hence, taking this parameterization as a basis, we generate eight additional exposure datasets
combining values of m and n taken from a list: $m, n \in (0.75, 1, 1.25)$, assuming variations of $\pm 25\%$ in the m and n parameters
240 to lead to reasonable variations in the generated exposure dataset. The parameter f_{exp} represents the choice of the exposure
dataset, and is uniformly drawn over nine index values: $f_{exp} \in (0, 1, 2, ..., 8)$, assuming all generated exposure layer to be
equally plausible. We quantify the uncertainty associated with the vulnerability by using two different impact functions to
model the damages: the Sw2010 and the CubEOT impact functions, as this allows us to account for the uncertainty associated
with the functional form of the impact function used to model the damages. The parameter $impfid$ represents the choice of
245 the impact function and is drawn uniformly over the two possible index values $impfid \in (0, 1)$, as we consider both functions
to be equally valid choices. Important uncertainties can also arise as a result of the calibration of an impact function. We
estimate those uncertainties by perturbing the input-intensity and output-MDD scales of the impact functions with two separate
multiplicative factors x_{scale} and y_{scale}, which we draw separately from a uniform distribution $x_{scale}, y_{scale} \in [0.80, 1.20]$. We
choose boundaries for the uncertainty parameters of 0.80 and 1.20 as we estimate an error of $\pm 20\%$ to be a reasonable estimate
250 of the error occurring in the modelling of European winter storms damages (Prahl et al., 2012).

We select the variance-based Sobol´ sensitivity indices as sensitivity metrics (Sobol, 2001). Using the quasi Monte Carlo
sampling scheme and the computation methodology described in Saltelli et al. (2010), we generate 32768 samples and compute
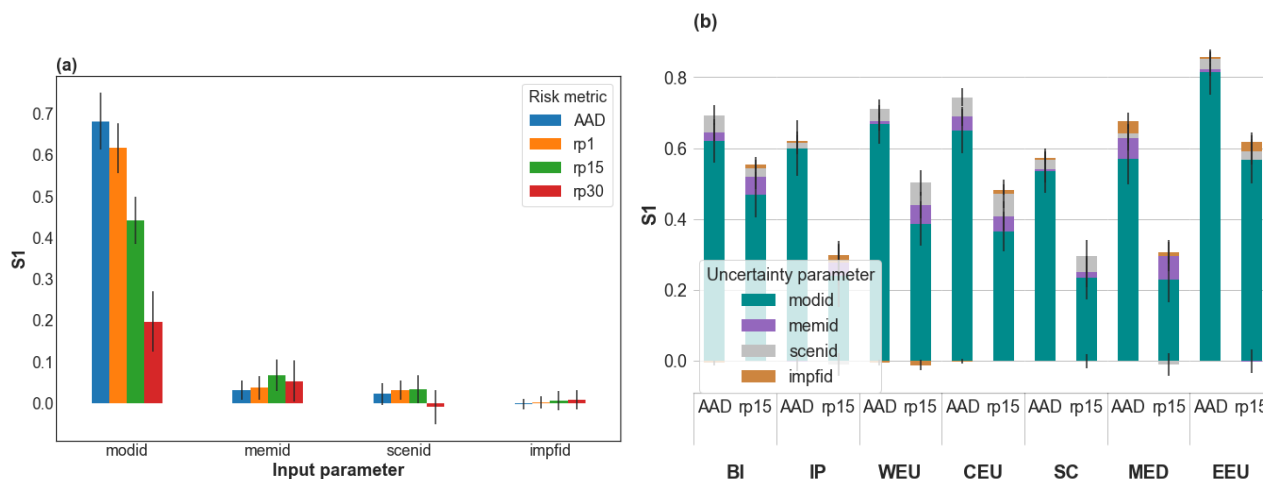
Figure 4. First order Sobol′ sensitivity indices (S1) for the future-minus-historical change relative to the historical period (delta climate) in winter storm damage in Europe, comparing a future (2070-2100) to a historical period (1980-2010). Panel **(a)** shows results for the delta climate change in average annual damage (AAD), and in damage amounts with return periods of one, 15, and 30 years (rp1, rp15, and rp30), aggregated over all exposure points of the entire European domain; Panel **(b)** shows results for the delta climate change in average annual damage (AAD), and in damage amount with a return periods of 15 years (rp15), aggregated over all exposure points in each of the seven regions defined in Fig. 2: British Isles (BI), Iberian Peninsula (IP), Western Europe (WEU), Central Europe (CEU), Mediterranean and Balkan region (MED), Scandinavia (SC), and Eastern Europe (EEU). The uncertainty factors (cf. sec. 2.6) are $modid$: climate model choice, $memid$: climate model member choice, $scenid$: future climate scenario choice, and $impfid$: impact function choice. The vertical black bars in **(a)** and **(b)** indicate the 95th percentile confidence intervals.

first order (S1), and total order (ST) Sobol´ sensitivity indices for several damage and risk metrics. First order Sobol´ sensitivity indices represent the direct contribution of a model's uncertainty factors to the model output variance. Total order Sobol´ sensitivity indices represent the sensitivity to a factor including all its higher order interactions with the other uncertainty factors.

3 Results

We first conduct a sensitivity analysis to determine the dominant factors of uncertainty in the projection of future changes in winter windstorm damage. Secondly, we present the future changes in winter windstorm damage, using the findings of the sensitivity analysis to restrict the analysis to the components of the projection ensemble which are the most relevant for the uncertainty in the projections.

3.1 Sensitivity analysis

We conduct a sensitivity analysis using Sobol´ sensitivity indices to determine the most relevant uncertainty factors for projections of future changes in winter storm damage in Europe. We determine the leading uncertainty factors at a continental scale and study the influence of considering damage events with increasingly longer return periods on the sensitivity. To do so, we investigate sensitivity on the average annual damage, and on damage amounts with return periods of one, 15, and 30 years, aggregated over the entire domain. As a second step, we assess whether the results of the sensitivity analysis vary according to the region considered, by considering sensitivity on the average annual damage and on damage amounts with return periods of 15 years, aggregating over the seven different sub-regions defined in Fig. 2. We consider for our sensitivity analysis relative changes in the damage and risk metrics, where relative refers to the future-minus-historical changes of the metrics with respect to the historical period.

Fig. 4a displays first order Sobol´ sensitivity indices (S1) for the Average Annual Damage (AAD), and for damages corresponding to return periods of one, 15, and 30 years (rp1, rp15, rp30), aggregated over the entire domain. Confidence intervals obtained by bootstrapping are plotted to inform on the precision of the estimated sensitivity indices and on the convergence of the sensitivity calculation. The confidence intervals indicate that the number of samples is sufficient to reach convergence and to obtain sufficiently precise estimates of the sensitivity indices. The values of the first order sensitivity indices indicate that the choice of the climate model ($modid$) is alone responsible for almost 70% of the total variance of the projection ensemble for the average annual damage. Climate model uncertainty also accounts for about 60%, and 45% of the total variance for damage amounts with return periods of respectively one and 15 years, but the contribution of this uncertainty factor drops to 20% for damage amounts with return periods of 30 years. The uncertainty associated with the use of different ensemble members ($memid$) ranks second, with values of the first order sensitivity indices not exceeding 10%, and the uncertainty associated with the future climate scenario ($scenid$) ranks third, with values of the first order sensitivity indices not exceeding 5%. Therefore, climate model uncertainty is the dominant uncertainty for average annual damage and damage amounts with return periods up to 15 years when aggregating the results to the entire domain. Overall, the first order sensitivities to the impact function calibration factors x_{scale}, and y_{scale}, and to the exposure layer f_{exp} are negligible for the four damage metrics here considered. Those three parameters were thus removed from Fig. 4a and b, and are ignored in the further analyses. Complete figures including the uncertainty contribution from the x_{scale}, y_{scale}, and f_{exp} parameters can be found in the appendix (Fig. B1). For damages with return periods higher than 15 years, the sum of all first order sensitivity indices drops below 50%, indicating that interactions between the different uncertainty factors become more important than the direct contributions of the uncertainty factors taken separately (Saltelli, 2002). We explain this increasing importance of interactions between uncertainty factors by the sampling uncertainty associated with increasing return periods. In our modelling framework, damages with return periods of 15 years and higher are based on two and one damage events respectively, which renders the estimation of the damage metrics highly influenced by sampling uncertainty. In consequence, the sensitivity analysis cannot clearly separate the contributions of the different uncertainty factors, as those become confounded with the sampling uncertainty.

Alternatively, we examine total order Sobol´ sensitivity indices (ST), as those indices inform on the total contribution of an uncertainty factor to the uncertainty, including all the interactions with the other uncertainty factors (Fig. 4a). The total order sensitivity indices also emphasize the dominance of the climate model uncertainty, as the total order sensitivity indices for the $modid$ parameter are systematically higher than the total order sensitivity indices for the other uncertainty factors. Therefore,

300   the climate model uncertainty remains the dominant uncertainty factor for damages with return periods of 15 years and higher. The choice of the ensemble member ($memid$), of the future climate scenario ($scenid$), and of the impact function ($impfid$) rank respectively second, third and fourth in terms of total order sensitivity. Interestingly, the values of the total order sensitivity indices increase with the return period for the $memid$, $scenid$, and $impfid$ parameters, but slightly decrease with the return period for the $modid$ parameter. This increase of the total order sensitivity indices with the return period suggests an increasing

305   importance of the $memid$, $scenid$, and $impfid$ uncertainty factors when investigating damages with increasing return periods.

We test the assumption that interactions between the uncertainty parameters are indeed associated with the sampling uncertainty by repeating the sensitivity analysis, but combining the three ensemble members from each climate model instead of considering the different ensemble members separately. Combining the different ensemble members of a climate model

310   instead of considering the members separately allows us to decrease the sampling uncertainty. The results of the sensitivity analysis obtained when considering the 90 years of modelled climate instead of separate 30 year periods are shown in Fig. B2. In contrast with the results of the sensitivity analysis obtained when considering the ensemble members separately, the sum of the first order sensitivity indices increases, indicating that considering longer time periods indeed helps to decrease the interactions between the uncertainty factors. In addition, we observe that climate model uncertainty remains the dominant source

315   of uncertainty for projections of damage amounts with return periods up to 30 years as the first order sensitivity index to the climate model is larger than 0.5 for the rp30 metric. Furthermore, the total and first order sensitivities to both the future climate scenario and impact function choice decrease when considering the combined simulations. This decrease indicates that the apparent increasing contribution of the future climate scenario and impact function uncertainty when considering damages with increasing return periods is at least partly associated with sampling uncertainty. Thus, the increasing relevance of the impact

320   function and future climate scenario should not be over-interpreted, as this increase is likely associated with the inability of the sensitivity quantification framework to differentiate between the different uncertainty factors when assessing damages with increasing return periods.

The sensitivity analysis conducted on the average annual damage and damage amounts with a return period of 15 years aggregated to the seven regions reveals that climate model uncertainty also dominates the uncertainty at a regional scale, as the values

325   of the first order sensitivity indices for the $modid$ parameter are systematically the highest in all regions (Fig.4b). Similarly as for the sensitivity analysis conducted for the results aggregated to the entire domain, the sums of the first order sensitivity indices decrease when damages with longer return periods (here rp15) are considered. We also note some inter-regional variations. For instance, the sensitivity to the impact function is higher in the Mediterranean region than in the other regions, when considering the average annual damage. This regional variability in the sensitivity to the impact function suggests that

330   the design of the impact function can become an increasingly important factor of uncertainty when assessing damages at a

regional level. However, we remind that this regional variability should be interpreted with care, as the effects of sampling uncertainty can be expected to increase when investigating smaller spatial scales.

Overall, our results emphasize the dominance of the climate model uncertainty when investigating future changes in winter windstorm damage over Europe. However, the sensitivity quantification framework which we use does not allow us to clearly

335   separate between the different sources of uncertainty when the return period of the estimated damage approaches the duration of the hazard dataset. Our findings are consistent with previous studies which also found the choice of the climate model to be a dominant factor of uncertainty for projections of future winter storm damage over Europe (e.g. Leckebusch et al., 2007; Pinto et al., 2007; Donat et al., 2011; Schwierz et al., 2010). In contrast, our analysis does not show the choice of the ensemble member or the future climate scenario to be important factors of uncertainty, which is partly in contradiction with

340   Donat et al. (2011) and Pinto et al. (2012). Using similar data but using a different uncertainty and sensitivity quantification method, Severino (2022) found the internal variability to become the dominant source of uncertainty when considering damage amounts with return periods of eight years and higher, indicating that the results are sensitive to the uncertainty and sensitivity quantification method used. We also do not find impact function uncertainty to be particularly relevant for our projections. However, we expect that considering changes in the damages in absolute terms should increase the importance of uncertainties

345   in the impact function, as the impact function is known to be a relevant factor of uncertainty in the assessment of winter storm damage (e.g. Koks and Haer, 2020).

3.2   Future changes in winter windstorm damage

The sensitivity analysis of the previous section highlighted the dominance of the climate model uncertainty on the projections of future changes in winter storm damage in Europe. In this section, we inspect spatial and regional changes in the damages

350   with a focus on the climate model spread. We consider a fixed impact function, Sw2010, a fixed future climate scenario, SSP585, and a fixed exposure data layer obtained with LitPop's base parameterization, as we showed the impact function, the future climate scenario, and the exposure distribution to be factors of uncertainty of minor importance in the previous section. We use spatial maps of the average annual damage resolved at the exposure level to study the spatial patterns in the damages. We then study the multi-model agreement in the projections of several damage metrics, and investigate the variation of the

355   multi-model agreement at a regional scale, by showing boxplots of the multi-model distributions of the average annual damage, and of damages with return periods of one, and 15 years, aggregated to the seven regions defined in Fig. 2. As before, we consider the changes in the damage metrics relative to the historical period.

We first investigate the spatial pattern of the change in the Average Annual Damage (AAD), as projected by the median of the multi-model ensemble of 30 GCMs (Fig. 5a). The multi-model median change shows increased future winter storm damages

360   within a band extending from the south of England to the Baltic states, throughout northern France, the Benelux, Denmark, Germany, and southern Sweden. In contrast, future storm damage is expected to decrease over northern Scandinavia and north-eastern Europe, as well as over the Iberian Peninsula and the Mediterranean. Parts of south-eastern Europe and the Balkan Peninsula also show a potential increase in the damages for the future period, although the signal is weaker and more scattered. The hatching on Fig. 5a highlights regions where 75% or more of the climate models agree on the sign of the change in the
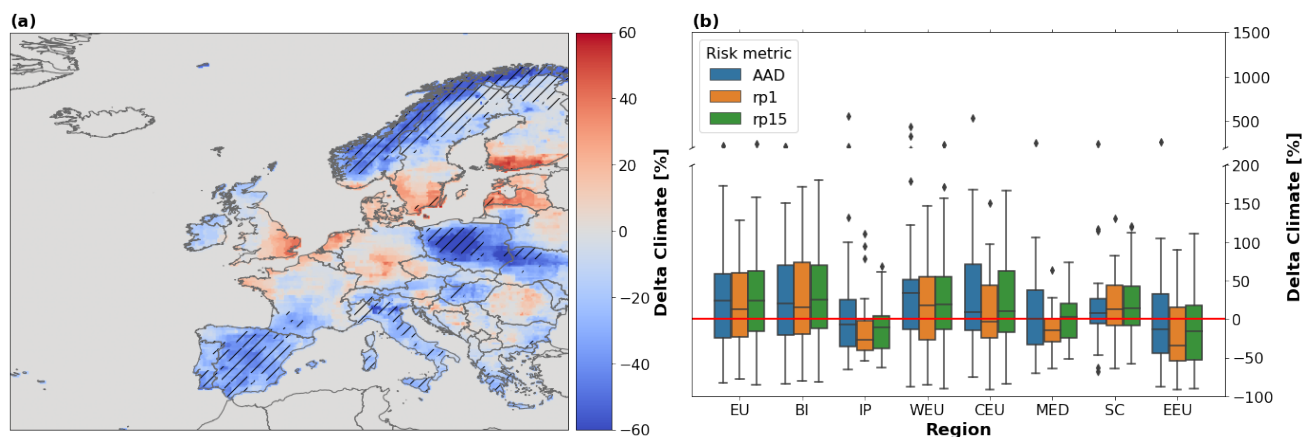
Figure 5. Regional changes in winter storm damage in Europe, comparing an SSP585 future (2070-2100) to a historical period (1980-2010), and using the impact function from Schwierz et al. (2010) to compute the damages. Panel **(a)** shows a spatial map of the multi-model median of the future-minus-historical change relative to the historical period (Delta Climate; %) in average annual damage, computed at each exposure point, where the hatching represents regions where more than 75% of the GCMs agree on the sign of the change in average annual damage; Panel **(b)** shows boxplots of the multi-model distributions of the future-minus-historical changes relative to the historical period (Delta Climate; %) in Average Annual Damage (AAD), and in damage amounts with return periods of one, and 15 years (rp1, rp15), aggregated over all exposure points in each of the seven regions defined in Fig. 2: British Isles (BI), Iberian Peninsula (IP), Western Europe (WEU), Central Europe (CEU), Mediterranean and Balkan region (MED), Scandinavia (SC), Eastern Europe (EEU), and over the entire European domain (EU). The boxplots' colored boxes represent the 25th and 75th percentile range (inter-quartile range) of the distributions, and the black lines inside the boxes represent the medians. The boxplot whiskers are drawn at distances of 1.5 times the inter-quartile range (IQR) below and above the 25th and 75th percentiles of the distributions or at the minimum and maximum data points when those points fall at a distance of less than 1.5 times the IQR. The diamonds represent outlying data points outside the whiskers. The red line represents the 0-% change line, which corresponds to no change in the future damages with respect to their historical value.

365 average annual damage. Overall, the climate models agree well over regions where a negative future change in the damages is expected (e.g. Iberian Peninsula, Italy, Poland, and northern Scandinavia). In contrast, the climate models tend to disagree over regions where a positive future change in the damages is expected, except over limited parts of southern Sweden, and western Latvia, where the model agreement reaches or exceeds 75%.

We investigate the multi-model spread at a regional scale, by examining boxplots of the multi-model distribution of the regional 370 changes in three damage metrics, the Average Annual Damage (AAD), and damage amounts with return periods of one and 15 years (rp1, rp15) in Fig. 5b. The boxplots' horizontal grey lines represent the medians, and the colored boxes the Inter-Quartile Ranges (IQR) of the regional distributions. The boxplots' whiskers represent either the minimum and maximum data points, or 1.5 times the IQR if the minimum and maximum data points fall beyond this distance. Data points falling beyond a distance of 1.5 times the IQR are represented by grey diamonds.

375 The boxplots confirm an important climate model uncertainty in all regions considered, with the boxplots' whiskers spanning

−80% to +170% in certain regions and for certain damage metrics. The 0%-change line is always covered by the colored boxes of the boxplots, indicating that the climate model agreement on the sign of the changes is always less than 75%, at the level of the regions considered. Disregarding the important spread, the multi-model medians of the ensemble show positive changes in the average annual damage in five regions: British Isles (BI, +20%), Western Europe (WEU, +34%), Central Europe (CEU, +9%), the Mediterranean and Balkan region (MED, +1%), and Scandinavia (SC, +8%); and negative changes in two regions: the Iberian Peninsula (IP,−7%), and Eastern Europe (EEU, −14%). When considering median changes in the damages aggregated to the entire domain, we observe a tendency for the damage amounts with longer return periods to increase more relatively to damages amounts with shorter return periods, as damage amounts with return periods of 15 years increase by +24%, while damage amounts with return periods of one year only increase by +13%. We recall that even small changes in the average annual damage might result in significant damage amounts, as the damages accumulate over the years. As an illustration, we show in absolute terms the future-minus-historical difference of the accumulated damages, resulting from the accumulation of 20 years of average annual damage over the historical and the future SSP585 period. The differences between the damages accumulated over 20 years of the historical period and the damages accumulated over 20 years of the future period yield +3.9 bn USD for the British Isles, +3.4 bn USD for Western Europe, +829 mn USD for Central Europe, +1.1 mn USD for the Mediterranean and Balkan region, +237 mn USD for Scandinavia, −107 mn USD for the Iberian Peninsula, and −29 mn USD for Eastern Europe, for a total of +6.9 bn USD for the entire European domain.

To better understand the spatial and regional patterns in the damages, we investigate the spatial patterns of changes for each individual climate model (not shown). While about half of the models project changes in extreme surface winds and damages consistent with an eastward extension of the North Atlantic storm track into Europe, the remaining models project changes in extreme surface winds which cannot be straightforwardly linked to such an extension of the storm track. Furthermore, using changes in the winter-half-year-averaged monthly-mean zonal winds at 850 hPa as a proxy for changes in the storm track location, we observe a potential link between the storm track tilt, and increased damages in the Balkan. Climate models showing an intensification of damages over Northern Europe tend to be linked to a southwesterly tilted intensification of the westerly winds, whereas models projecting damages in more southern locations are linked to a more westerly or northwesterly intensification of the westerly winds. This orientation of the low-level winds could then explain the increased surface winds in the Balkans, as those increased winds could be a consequence of enhanced lee cyclogenesis, resulting from the blocking of the flow by the Alpine ridge. However, verifying this theory would require a deeper investigation.

Our results are in agreement with the consensus of an eastward extension of the storm track into Europe, with numerous studies finding a similar pattern, using various data and methods (e.g., Pinto et al., 2007; Schwierz et al., 2010; Donat et al., 2011; Pinto et al., 2012). However, we find somewhat different results, in some regions, compared to other studies. For instance, Donat et al. (2011) and Pinto et al. (2012) find a pattern of damages extending over Poland, whereas we find a pattern of damages extending further north, with decreased damages over Poland. Furthermore, the potential increase of the damages in the Balkan region has not been observed in previous studies.
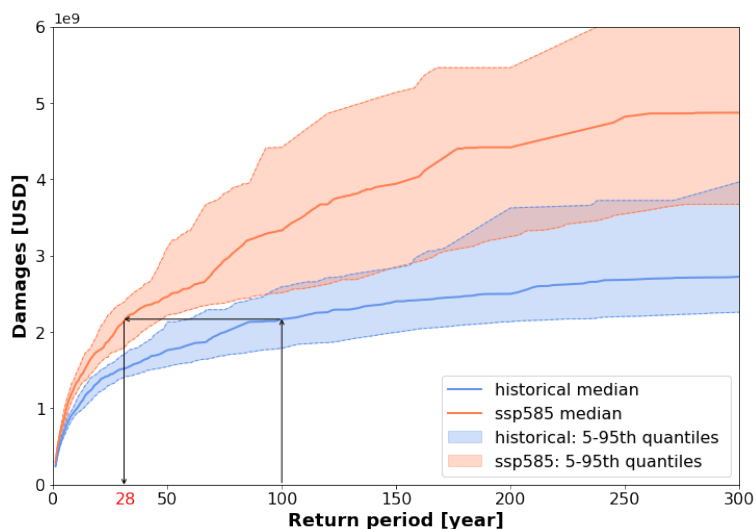
Figure 6. Exceedance Frequency Curves (EFCs) for future (2070-2100) SSP585 conditions, and historical (1980-2010) winter storm damage aggregated to the entire European domain. The EFCs are obtained using an ensemble of opportunity approach, combining the simulations from all the 30 climate models and their ensemble members, using the impact function from Schwierz et al. (2010). The effects of internal variability on the EFCs are simulated by generating multiple EFCs via bootstrapping. Solid lines represent the medians, and dashed lines the 5th and 95th percentiles of the distributions of the multiple EFCs generated via bootstrapping. The arrows highlight that the intensity of a damage event with a return period of 100 years under historical climate conditions corresponds to the intensity of a damage event with a return period of 28 years under future SSP585 climate conditions.

3.3 Ensemble of opportunity

In this section we investigate the future changes in extreme damage events with long return periods by taking an ensemble of opportunity approach. Figure 6 displays the Exceedance Frequency Curves (EFCs), computed for the historical and future SSP585 periods using the ensemble of opportunity. For each GCM and each study period (historical and future), we randomly sample with replacement storm days corresponding to 20 winter seasons, and combine those $20 \times 6 \times 30 = 3600$ months of data to one long simulation. Each EFC thus represents a random realization of 3600 winter months, corresponding to 600 winter seasons, and is obtained from an ensemble of 30 GCMs, where each GCM is equally represented. We estimate the effect of internal variability on the projections using a bootstrapping approach, where we generate 1000 random realizations of the EFCs, and compute approximate confidence intervals using 5th and 95th percentiles of the bootstrapped distribution.

The EFCs generated using the ensemble of opportunity approach reveal a considerable increase in future damages with respect to historical damages. On average, future damage events are 64% more damaging than historical damage events. This increase in intensity means that, for instance, damages with an expected return period of 100 years under current climate would have a return period of only 28 years under future climate conditions. The 90% confidence intervals of the historical and future curves show no overlap for damage amounts with return periods below 100 years, suggesting that the observed increase of future

damages is likely not to be a consequence of the internal variability in the projections, at least for damage amounts with return
periods below 100 years.

Our results are compatible with previous studies, as for instance with Schwierz et al. (2010), who found that damages with return periods of 100 years could increase by 50% to 150% for Europe's end-of-century climate, and with Pinto et al. (2012), who found a potential for the frequency of extreme damage events (i.e. with return periods of 50 or 100 years) to increase by a factor of about two to four.

4   Summary, discussion and conclusion

In this paper, we investigate future changes in winter storm damage risk over Europe, and assess the importance of diverse sources of uncertainty in the projections. We find large uncertainties in the projections of future changes in European winter windstorm damages, and climate model uncertainty to be the dominant factor of uncertainty in the projections. Using the median to measure the general tendency of a multi-model ensemble of 30 general circulation models, we find regional increases in winter storm damage risk over western, and northern-central Europe, and a decrease over the rest of Europe, in agreement with an eastward extension of the North Atlantic storm track into Europe. In particular, we highlight the British Isles and Western Europe to be particularly at risk, with the median of the multi-model ensemble projecting increases in average annual winter storm damage of +20% and +34%, respectively. We find more moderate increases in the damages in Central European (+9%), Scandinavian (+8%), and the Mediterranean and Balkan (+1%) regions, and decreases in the Iberian Peninsula (-7%) and Eastern European (-14%) regions. Overall, the climate model agreement on the future changes in winter storm damage is poor over the regions where the damages are expected to increase according to the multi-model median, but the climate model agreement improves over the regions where the damages are expected to decrease according to the multi-model median. We find evidence for the damages associated with long return periods to increase more relatively to damages associated with shorter return periods, with multi-model median European-wide damage amounts associated with return periods of one and 15 years increasing by +13% and +24% respectively. Using an ensemble of opportunity approach, we also find evidence for an increase in the intensity of future extreme damage events, with for instance damages associated with return periods of 100 years under current climate becoming damages associated with return periods of only 28 years under future SSP585 climate conditions.

Overall, our results are consistent with previous studies that assessed future changes in winter storm damage risk over Europe, using global or regional climate models. The spatial and regional patterns of damages that we find are in line with an eastward extension of the North Atlantic storm track into Europe in winter, consistent with findings based on previous CMIP phases (for CMIP5, see e.g. Zappa et al., 2013). However, we emphasize that the projections of future storm damage are highly dependent on the climate model chosen, and that not all climate models show changes in extreme surface wind speeds and wind damages consistent with an eastward extension of the North Atlantic storm track. The substantial disagreement of the GCMs on the pattern of future changes of extreme surface winds over Europe in winter is not surprising, given the known difficulties of low-resolution climate models to simulate extratropical cyclones (Seneviratne et al., 2021), and to represent regional

circulation patterns and their changes (Zappa and Shepherd, 2017; Fernandez-Granja et al., 2021). Our results thus emphasize a significant disagreement on the future changes in extreme surface winds over Europe among the climate models participating in CMIP6, consistent with the findings of Kumar et al. (2015), who highlighted large inter-model differences in projections of extreme surface winds among CMIP5 climate models.

460

From a risk management perspective, our uncertainty and sensitivity analysis can provide valuable information for decision makers interested in the assessment of the future risks of winter windstorm damage in Europe. Our findings highlight the climate model uncertainty to be a key factor of uncertainty, and we encourage actors in the risk management sector to account for this factor in their decision process. In particular, we suggest risk-friendly decision makers to base their decisions on projections from climate models which are close to the median of the multi-model ensemble, or on the median of the projections directly. On the other hand, we suggest risk-averse decision makers to base their decisions on climate models which are projecting more significant increases in future winter windstorm damage, by for instance selecting climate models whose projections are close to the 90th percentile of the multi-model ensemble. To help decision makers in selecting climate model projections appropriated to their need, we rank the 30 climate models according to their projected future change in average annual damage in Tab. A1.

465

470

Addressing the shortcomings of our study, we should emphasize that our uncertainty and sensitivity analysis only covers part of the uncertainty associated with the modelling of winter windstorm damage in a future climate. Other potentially important uncertainty factors might have been missed, either because we choose not to include them (e.g. storm day detection uncertainty), or because we were not aware of them (on the concept of *unknown unknowns*, see e.g. Kundzewicz et al., 2018; Zumwald et al., 2020). Furthermore, we can expect our results to change when considering additional climate models and ensemble members, additional impact functions, or different distribution and values for the uncertainty factors. In particular, we note that the 14 climate models selected for the uncertainty and sensitivity quantification are probably not fully representing the climate model uncertainty associated with the ensemble of 30 climate models used for the damage projection of this study. Hence, the uncertainty we quantify in this study is likely only a partial representation of the overall uncertainty. This imperfect depiction of the uncertainty should be borne in mind when interpreting the confidence intervals or uncertainty estimates we derive in this study.

475

480

In addition, we found that the surface wind maxima outputs from some of the GCMs considered in this study were subjected to significant biases when compared to the ERA5 reanalysis. While we could partly overcome this limitation by conducting a bias-correction based on percentile mapping, we expect that using an approach based on dynamical downscaling could bring significant improvements in the damage estimations (see e.g. the EURO-CORDEX project; Jacob et al., 2014). Using a dynamical downscaling approach should improve the biases in the representation of extreme surface winds, especially over regions with complex topography, and allow to obtain more accurate and spatially refined estimates of the future changes in extreme winds and wind damages.

485

490

To our knowledge, our study is the first quantification of projected future changes and the uncertainty of winter windstorm damage that covers such an extensive number of CMIP6 models, and which investigates uncertainty associated with modelling of the hazard, the exposure, and the vulnerability. As it stands, the large climate model disagreement in the future changes of extreme surface winds over Europe is the limiting factor in the projections of future winter windstorm damage over Europe. This large disagreement must be reduced in order for the impact of climate change on future winter windstorm damage in Europe to be successfully assessed. Our findings thus motivate further research and efforts aimed at improving the representation of windstorms and the European winter climate by general circulation models. Additionally, our study emphasizes the benefits of using large ensembles of climate models for climate impact assessment studies to obtain optimal estimates of projected climate impacts. Our study also provides a common framework that can serve as guidance for future climate risk assessment studies, where a large ensemble of GCMs' projections is successfully combined with an open-source and user-friendly weather and climate risk assessment model such as CLIMADA.

Code availability. CLIMADA is openly available at GitHub https://github.com/CLIMADA-project/climada_python (last access: 23 December 2022), and https://doi.org/10.5281/zenodo.5947271 (gabrielaznar et al., 2022) under the GNU GPL license (GNU operating system, 2007). The documentation is hosted on Read the Docs https://climada-python.readthedocs.io/en/stable/ (last access: 23 December 2022) and includes a link to the interactive tutorial of CLIMADA. In this publication, CLIMADA v3.2.0, deposited on Zenodo (gabrielaznar et al., 2022) was used.

Author contributions. All authors contributed to conceptualization; data curation, formal analysis, visualization, and writing of the original draft was by Luca G. Severino; writing – review and editing – was by Luca G. Severino, Chahan M. Kropf, Hilla Afargan-Gerstman, Andries Jan de Vries, Daniela I.V. Domeisen, and David N. Bresch; supervision was by Chahan M. Kropf, Hilla Afargan-Gerstman, Christopher Fairless, Andries Jan de Vries, Daniela I.V. Domeisen, and David N. Bresch; project administration was by Daniela I.V. Domeisen and David N. Bresch.

Competing interests. The authors declare that they have no conflict of interest.

Acknowledgements. We acknowledge the World Climate Research Programme for coordinating and promoting CMIP6 through its Working Group on Coupled Modelling. We acknowledge the work of the climate modelling groups participating in CMIP6, who produced and made available their model output, and we thank the Earth System Grid Federation for archiving the data and providing access. Hilla Afargan-Gerstman acknowledges funding from the European Union's Horizon 2020 research and innovation programme under the Marie Skłodowska-Curie grant agreement No 891514. Support from the Swiss National Science Foundation through project PP00P2_198896 to

Daniela I.V. Domeisen is gratefully acknowledged. This project has received funding from the European Union's Horizon 2020 research and innovation programme under grant agreements No 821010 and No 820712.

Appendix A: Methods

Table A1. Variant names, nominal resolution (Nominal res. (km)), and future-minus-historical change relative to the historical period in the average annual damage (AAD change (%)) of the different climate models considered in this study. The x symbol denotes missing ensemble member.

	Variant name						Nominal res.	AAD change
Future climate scenario	historical			ssp585			(km)	(%)
Ensemble member id	0	1	2	0	1	2		
Climate model								
GFDL-CM4	r1i1p1f1	x	x	r1i1p1f1	x	x	100	544.6
CMCC-CM2-SR5	r1i1p1f1	x	x	r1i1p1f1	x	x	100	217.4
ACCESS-CM2	r4i1p1f1	r5i1p1f1	x	r4i1p1f1	r5i1p1f1	x	250	172.3
CNRM-CM6-1-HR	r1i1p1f2	x	x	r1i1p1f2	x	x	50	127.0
CMCC-ESM2	r1i1p1f1	x	x	r1i1p1f1	x	x	100	78.8
MPI-ESM1-2-HR	r1i1p1f1	r2i1p1f1	x	r1i1p1f1	r2i1p1f1	x	100	71.3
MIROC-ES2L	r1i1p1f2	r2i1p1f2	r3i1p1f2	r1i1p1f2	r2i1p1f2	r3i1p1f2	500	68.9
GISS-E2-1-G	r1i1p1f2	x	x	r1i1p1f2	x	x	250	58.3
HadGEM3-GC31-LL	r1i1p1f3	r2i1p1f3	r3i1p1f3	r1i1p1f3	r2i1p1f3	r3i1p1f3	250	58.1
MPI-ESM1-2-LR	r1i1p1f1	r2i1p1f1	r3i1p1f1	r1i1p1f1	r2i1p1f1	r3i1p1f1	250	50.1
BCC-CSM2-MR	r1i1p1f1	x	x	r1i1p1f1	x	x	100	44.9
CNRM-CM6-1	r1i1p1f2	r2i1p1f2	r3i1p1f2	r1i1p1f2	r2i1p1f2	r3i1p1f2	250	41.1
MRI-ESM2-0	r1i1p1f1	r2i1p1f1	r3i1p1f1	r1i1p1f1	r2i1p1f1	r3i1p1f1	100	35.6
EC-Earth3-CC	r1i1p1f1	x	x	r1i1p1f1	x	x	100	29.7
MIROC6	r1i1p1f1	r2i1p1f1	r3i1p1f1	r1i1p1f1	r2i1p1f1	r3i1p1f1	250	27.3
IPSL-CM6A-LR	r1i1p1f1	r2i1p1f1	r3i1p1f1	r1i1p1f1	r2i1p1f1	r3i1p1f1	250	19.7
ACCESS-ESM1-5	r1i1p1f1	r2i1p1f1	r3i1p1f1	r1i1p1f1	r2i1p1f1	r3i1p1f1	250	5.9
FGOALS-g3	r1i1p1f1	r3i1p1f1	r4i1p1f1	r1i1p1f1	r3i1p1f1	r4i1p1f1	250	5.8
HadGEM3-GC31-MM	r1i1p1f3	r2i1p1f3	r3i1p1f3	r1i1p1f3	r2i1p1f3	r3i1p1f3	100	4.0
AWI-CM-1-1-MR	r1i1p1f1	x	x	r1i1p1f1	x	x	100	-2.6
CNRM-ESM2-1	r1i1p1f2	r4i1p1f2	r5i1p1f2	r1i1p1f2	r4i1p1f2	r5i1p1f2	250	-6.7
UKESM1-0-LL	r1i1p1f2	r2i1p1f2	r3i1p1f2	r1i1p1f2	r2i1p1f2	r3i1p1f2	250	-16.5
NESM3	r1i1p1f1	~~r2i1p1f1~~	x	r1i1p1f1	~~r2i1p1f1~~	x	250	-27.2
CanESM5	r1i1p1f1	r2i1p1f1	r3i1p1f1	r1i1p1f1	r2i1p1f1	r3i1p1f1	500	-28.1
EC-Earth3-Veg	r1i1p1f1	r2i1p1f1	r3i1p1f1	r1i1p1f1	r2i1p1f1	r3i1p1f1	100	-32.9
EC-Earth3	r1i1p1f1	r3i1p1f1	r4i1p1f1	r1i1p1f1	r3i1p1f1	r4i1p1f1	100	-32.9
EC-Earth3-Veg-LR	r1i1p1f1	r2i1p1f1	r3i1p1f1	r1i1p1f1	r2i1p1f1	r3i1p1f1	100	-35.1
INM-CM5-0	r1i1p1f1	x	x	r1i1p1f1	x	x	100	-35.1
INM-CM4-8	r1i1p1f1	x	x	r1i1p1f1	x	x	100	-44.7
KACE-1-0-G	r1i1p1f1	r2i1p1f1	r3i1p1f1	r1i1p1f1	r2i1p1f1	r3i1p1f1	250	-82.5

Table A2. Variant names of the additional ensemble members used for the uncertainty and sensitivity analysis using the SSP126, SSP245, and SSP370 experiments.

	Variant name								
Future climate scenario		ssp126			ssp245			ssp370	
Ensemble member id	0	1	2	0	1	2	0	1	2
Climate model									
CanESM5	r1i1p1f1	r2i1p1f1	r3i1p1f1	r1i1p1f1	r2i1p1f1	r3i1p1f1	r1i1p1f1	r2i1p1f1	r3i1p1f1
CNRM-CM6-1	r1i1p1f2	r2i1p1f2	r3i1p1f2	r1i1p1f2	r2i1p1f2	r3i1p1f2	r1i1p1f2	r2i1p1f2	r3i1p1f2
CNRM-ESM2-1	r1i1p1f2	r4i1p1f2	r5i1p1f2	r1i1p1f2	r4i1p1f2	r5i1p1f2	r1i1p1f2	r4i1p1f2	r5i1p1f2
EC-Earth3-Veg	r1i1p1f1	r2i1p1f1	r3i1p1f1	r1i1p1f1	r2i1p1f1	r3i1p1f1	r1i1p1f1	r2i1p1f1	r3i1p1f1
EC-Earth3-Veg-LR	r1i1p1f1	r2i1p1f1	r3i1p1f1	r1i1p1f1	r2i1p1f1	r3i1p1f1	r1i1p1f1	r2i1p1f1	r3i1p1f1
IPSL-CM6A-LR	r1i1p1f1	r2i1p1f1	r3i1p1f1	r1i1p1f1	r2i1p1f1	r3i1p1f1	r1i1p1f1	r2i1p1f1	r3i1p1f1
MIROC-ES2L	r1i1p1f2	r2i1p1f2	r3i1p1f2	r1i1p1f2	r2i1p1f2	r3i1p1f2	r1i1p1f2	r2i1p1f2	r3i1p1f2
UKESM1-0-LL	r1i1p1f2	r2i1p1f2	r3i1p1f2	r1i1p1f2	r2i1p1f2	r3i1p1f2	r1i1p1f2	r2i1p1f2	r3i1p1f2
MRI-ESM2-0	r1i1p1f1	r2i1p1f1	r3i1p1f1	r1i1p1f1	r2i1p1f1	r3i1p1f1	r1i1p1f1	r2i1p1f1	r3i1p1f1
FGOALS-g3	r1i1p1f1	r3i1p1f1	r4i1p1f1	r1i1p1f1	r3i1p1f1	r4i1p1f1	r1i1p1f1	r3i1p1f1	r4i1p1f1
ACCESS-ESM1-5	r1i1p1f1	r2i1p1f1	r3i1p1f1	r1i1p1f1	r2i1p1f1	r3i1p1f1	r1i1p1f1	r2i1p1f1	r3i1p1f1
MIROC6	r1i1p1f1	r2i1p1f1	r3i1p1f1	r1i1p1f1	r2i1p1f1	r3i1p1f1	r1i1p1f1	r2i1p1f1	r3i1p1f1
MPI-ESM1-2-LR	r1i1p1f1	r2i1p1f1	r3i1p1f1	r1i1p1f1	r2i1p1f1	r3i1p1f1	r1i1p1f1	r2i1p1f1	r3i1p1f1
KACE-1-0-G	r1i1p1f1	r2i1p1f1	r3i1p1f1	r1i1p1f1	r2i1p1f1	r3i1p1f1	r1i1p1f1	r2i1p1f1	r3i1p1f1

Figure A1. Physical assets distribution measured in USD, obtained by combining population density layer and nightlight satellite imagery, using produced capital as the macroeconomic indicator and using the base parameterization of LitPop (cf. Litpop method Eberenz et al., 2020).

Appendix B: Results

B1 Uncertainty and sensitivity analysis
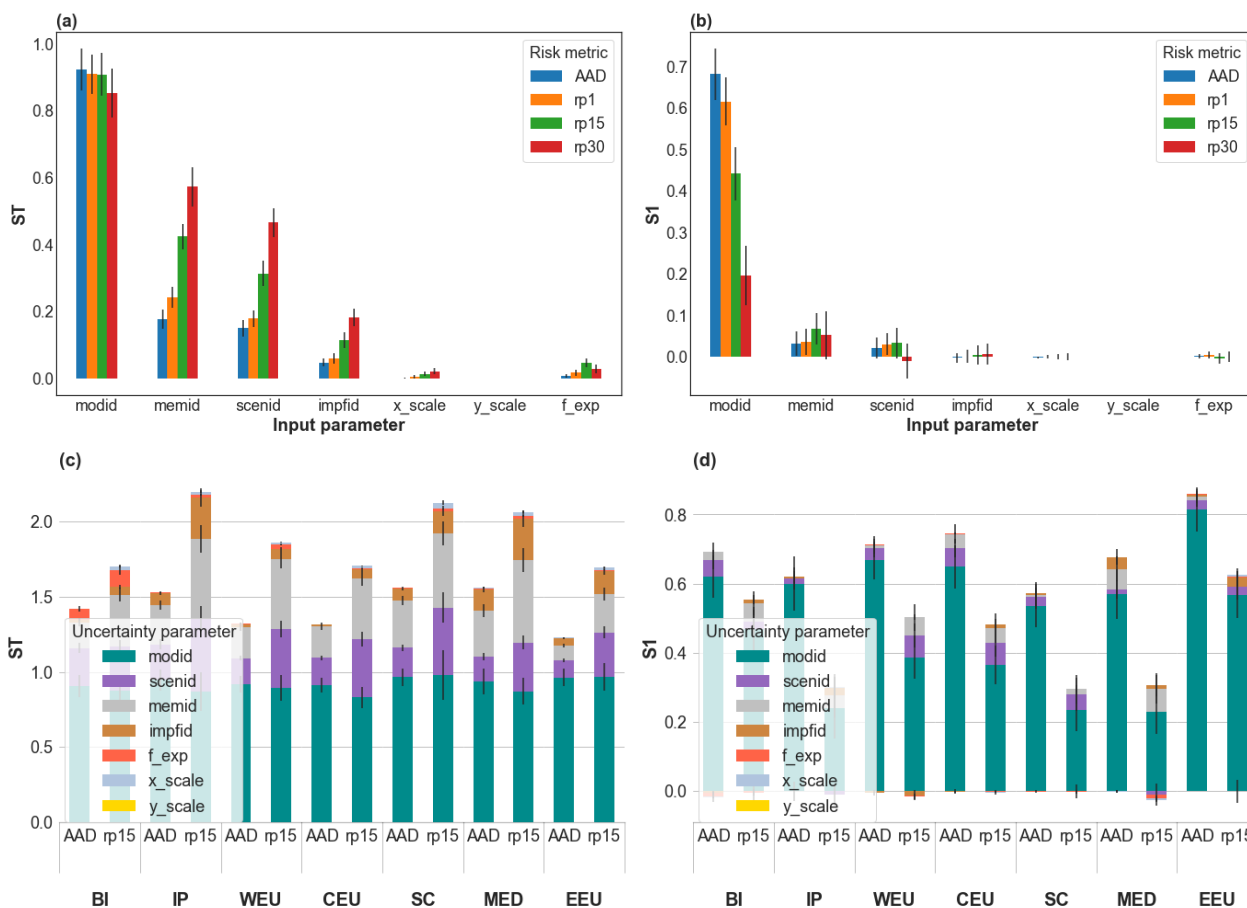
Figure B1. Total and first order Sobol′ sensitivity indices (ST, S1) for the future-minus-historical change relative to the historical period (delta climate) in winter storm damage in Europe, comparing a future (2070-2100) to a historical period (1980-2010). Panels **(a)** and **(b)** respectively show ST and S1 indices for the delta climate change in average annual damage (AAD), and in damage amounts with return periods of one, 15, and 30 years (rp1, rp15, and rp30), aggregated over all exposure points of the entire European domain; **(c)** and **(d)** respectively show ST and S1 indices for the delta climate change in average annual damage (AAD), and in damage amount with a return periods of 15 years (rp15), aggregated over all exposure points in each of the seven regions defined in Fig. 2: British Isles (BI), Iberian Peninsula (IP), Western Europe (WEU) Central Europe (CEU), Mediterranean and Balkan region (MED), Scandinavia (SC), and Eastern Europe (EEU). The uncertainty factors (cf. sec. 2.6) are $modid$: climate model choice, $scenid$: future climate scenario choice, $memid$: climate model member choice, $impfid$: impact function choice, x_{scale}: impact function input intensity scaling factor, y_{scale}: impact function output MDD scaling factor, and f_{exp}: the exposure layer choice. The vertical black bars in **(a)**, **(b)**, **(c)**, and **(d)** indicate the 95th percentile confidence intervals.
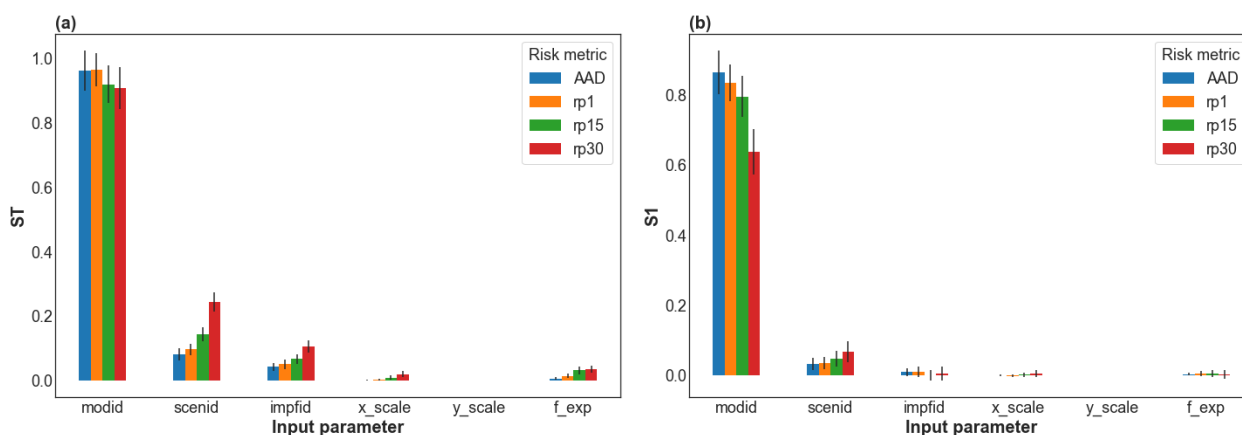
Figure B2. Total and first order Sobol′sensitivity indices (ST, S1) for the future-minus-historical change relative to the historical period (delta climate) in winter storm damage in Europe, comparing a future (2070-2100) to a historical period (1980-2010), and combining members from the climate models into single 90 years simulations. Panels **(a)** and **(b)** respectively show ST and S1 indices for the delta climate change in average annual damage (AAD), and in damage amounts with return periods of one, 15, and 30 years (rp1, rp15, and rp30), aggregated over all exposure points of the entire European domain. The uncertainty factors (cf. sec. 2.6) are $modid$: climate model choice, $scenid$: future climate scenario choice, $impfid$: impact function choice, x_{scale}: impact function input intensity scaling factor, y_{scale}: impact function output MDD scaling factor, and f_{exp}: the exposure layer choice. The vertical black bars in **(a)** and **(b)** indicate the 95th percentile confidence intervals.

References

525 Aznar-Siguan, G. and Bresch, D. N.: CLIMADA v1: A global weather and climate risk assessment platform, Geosci. Model Dev., 12, 3085–3097, https://doi.org/10.5194/gmd-12-3085-2019, 2019.

Catto, J. L., Ackerley, D., Booth, J. F., Champion, A. J., Colle, B. A., Pfahl, S., Pinto, J. G., Quinting, J. F., and Seiler, C.: The Future of Midlatitude Cyclones, Curr. Clim. Chang. Rep., 5, 407–420, https://doi.org/10.1007/s40641-019-00149-4, 2019.

Christensen, J. H. and Christensen, O. B.: A summary of the PRUDENCE model projections of changes in European climate by the end of 530 this century, Climatic Change, 81, 7–30, https://doi.org/10.1007/s10584-006-9210-7, 2007.

Della-Marta, P. M., Liniger, M. A., Appenzeller, C., Bresch, D. N., Köllner-Heck, P., and Muccione, V.: Improved estimates of the European winter windstorm climate and the risk of reinsurance loss using climate model data, J. Appl. Meteor. Climatol., 49, 2092–2120, https://doi.org/10.1175/2010JAMC2133.1, 2010.

Donat, M. G., Leckebusch, G. C., Pinto, J. G., and Ulbrich, U.: Examination of wind storms over Central Europe with respect to circulation 535 weather types and NAO phases, Int. J. Climatol., 30, 1289–1300, https://doi.org/10.1002/joc.1982, 2010a.

Donat, M. G., Leckebusch, G. C., Wild, S., and Ulbrich, U.: Benefits and limitations of regional multi-model ensembles for storm loss estimations, Clim. Res., 44, 211–225, https://doi.org/10.3354/cr00891, 2010b.

Donat, M. G., Leckebusch, G. C., Wild, S., and Ulbrich, U.: Future changes in European winter storm losses and extreme wind speeds inferred from GCM and RCM multi-model simulations, Nat. Hazards Earth Syst. Sci., 11, 1351–1370, https://doi.org/10.5194/nhess-11- 540 1351-2011, 2011.

Eberenz, S., Stocker, D., Röösli, T., and Bresch, D. N.: Asset exposure data for global physical risk assessment, Earth Syst. Sci. Data, 12, 817–833, https://doi.org/10.5194/essd-12-817-2020, 2020.

Eyring, V., Bony, S., Meehl, G. A., Senior, C. A., Stevens, B., Stouffer, R. J., and Taylor, K. E.: Overview of the Coupled Model Intercomparison Project Phase 6 (CMIP6) experimental design and organization, Geosci. Model Dev., 9, 1937–1958, https://doi.org/10.5194/gmd- 545 9-1937-2016, 2016.

Fernandez-Granja, J. A., Casanueva, A., Bedia, J., and Fernandez, J.: Improved atmospheric circulation over Europe by the new generation of CMIP6 earth system models, Clim. Dyn., 56, 3527–3540, https://doi.org/10.1007/s00382-021-05652-9, 2021.

gabrielaznar, Eberenz, S., Vogt, T., Schmid, E., Steinmann, C. B., Yu, Y., Röösli, T., Lüthi, S., Sauer, I. J., Mühlhofer, E., Hartman, J., Kropf, C. M., Guillod, B. P., Stalhandske, Z., Ciullo, A., Bresch, D. N., Fairless, C., Kam, P. M. M., wjan262, Riedel, L., Meiler, S., Rachel_B, 550 veronicabozzini, and DarioStocker: CLIMADA-project/climada_python: v3.2.0, https://doi.org/10.5281/zenodo.6807463, 2022.

Guha-Sapir, D.: EM-DAT, CRED / UCLouvain, Brussels, Belgium, www.emdat.be, (last access: 13 November 2021), 2021.

Harvey, B. J., Cook, P., Shaffrey, L. C., and Schiemann, R.: The Response of the Northern Hemisphere Storm Tracks and Jet Streams to Climate Change in the CMIP3, CMIP5, and CMIP6 Climate Models, J. Geophys. Res. Atmos., 125, https://doi.org/10.1029/2020JD032701, 2020.

555 Haylock, M. R.: European extra-tropical storm damage risk from a multi-model ensemble of dynamically-downscaled global climate models, Nat. Hazards Earth Syst. Sci., 11, 2847–2857, https://doi.org/10.5194/nhess-11-2847-2011, 2011.

Heneka, P., Hofherr, T., and Ruck, B.: Winter storm risk in Germany under climate change, in: 8. Forum DKKV/CEDIM: Disaster Reduction in Climate Change 15./16.10.2007, Karlsruhe University, https://www.researchgate.net/publication/237631041, 2007.

Hochman, A., Marra, F., Messori, G., Pinto, J. G., Raveh-Rubin, S., Yosef, Y., and Zittis, G.: Extreme weather and societal impacts in the 560 eastern Mediterranean, Earth Syst. Dyn., 13, 749–777, https://doi.org/10.5194/esd-13-749-2022, 2022.

IPCC: Climate Change 2014: Impacts, Adaptation, and Vulnerability. Part A:Global and Sectoral Aspects. Contribution of Working Group II to the Fifth Assessment Report of the Intergovernmental Panel on Climate Change, vol. In Press, Cambridge University Press, Cambridge, United Kingdom and New York, NY, USA, https://www.ipcc.ch/report/ar5/syr/, (last access: 23 December 2022), 2014.

Jacob, D., Petersen, J., Eggert, B., Alias, A., Christensen, O. B., Bouwer, L. M., Braun, A., Colette, A., Déqué, M., Georgievski, G., Georgopoulou, E., Gobiet, A., Menut, L., Nikulin, G., Haensler, A., Hempelmann, N., Jones, C., Keuler, K., Kovats, S., Kröner, N., Kotlarski, S., Kriegsmann, A., Martin, E., van Meijgaard, E., Moseley, C., Pfeifer, S., Preuschmann, S., Radermacher, C., Radtke, K., Rechid, D., Rounsevell, M., Samuelsson, P., Somot, S., Soussana, J. F., Teichmann, C., Valentini, R., Vautard, R., Weber, B., and Yiou, P.: EURO-CORDEX: New high-resolution climate change projections for European impact research, Reg. Environ. Chang., 14, 563–578, https://doi.org/10.1007/s10113-013-0499-2, 2014.

Karremann, M. K., Pinto, J. G., Reyers, M., and Klawa, M.: Return periods of losses associated with European windstorm series in a changing climate, Environ. Res. Lett., 9, https://doi.org/10.1088/1748-9326/9/12/124016, 2014.

Klawa, M. and Ulbrich, U.: A model for the estimation of storm losses and the identification of severe winter storms in Germany, Nat. Hazards Earth Syst. Sci., 3, 725–732, https://doi.org/10.5194/nhess-3-725-2003, 2003.

Koks, E. E. and Haer, T.: A high-resolution wind damage model for Europe, Sci. Rep, 10, https://doi.org/10.1038/s41598-020-63580-w, 2020.

Kropf, C. M., Ciullo, A., Otth, L., Meiler, S., Rana, A., Schmid, E., McCaughey, J. W., and Bresch, D. N.: Uncertainty and sensitivity analysis for probabilistic weather and climate-risk modelling: an implementation in CLIMADA v.3.1.0, Geosci. Model Dev., 15, 7177–7201, https://doi.org/10.5194/gmd-15-7177-2022, 2022.

Kruschke, T.: Winter wind storms: Identification, verification of decadal predictions, and regionalization, Ph.D. thesis, Freien Universität Berlin, Berlin, https://www.researchgate.net/publication/281206536_Winter_wind_storms_Identification_verification_of_decadal_predictions_and_regionalization, (last access: 23 December 2022), 2014.

Kumar, D., Mishra, V., and Ganguly, A. R.: Evaluating wind extremes in CMIP5 climate models, Clim. Dyn., 45, 441–453, https://doi.org/10.1007/s00382-014-2306-2, 2015.

Kundzewicz, Z. W., Krysanova, V., Benestad, R. E., Hov, Piniewski, M., and Otto, I. M.: Uncertainty in climate change impacts on water resources, Environmental Science and Policy, 79, 1–8, https://doi.org/10.1016/j.envsci.2017.10.008, 2018.

Leckebusch, G. C., Ulbrich, U., Fröhlich, L., and Pinto, J. G.: Property loss potentials for European midlatitude storms in a changing climate, Geophys. Res. Lett., 34, https://doi.org/10.1029/2006GL027663, 2007.

Lee, J.-Y., Marotzke, J., Bala, G., Cao, L., Corti, S., Dunne, J., Engelbrecht, F., Fischer, E., Fyfe, J., Jones, C., Maycock, A., Mutemi, J., Ndiaye, O., Panickal, S., and Zhou, T.: Future Global Climate: Scenario-Based Projections and Near-Term Information, p. 553–672, Cambridge University Press, Cambridge, United Kingdom and New York, NY, USA, https://doi.org/10.1017/9781009157896.006, 2021.

Lüthi, S., Fairless, C., Fischer, E., Scovronick, N., Armstrong, B., Coelho, M., Guo, Y. L., Guo, Y., Honda, Y., Huber, V., Kyselý, J., Lavigne, E., Roye, D., and Ryti, N.: Rapid increase in the risk of heat-related mortality, Research Square, https://doi.org/10.21203/rs.3.rs-2190946/v1, 2022.

O'Neill, B. C., Tebaldi, C., Van Vuuren, D. P., Eyring, V., Friedlingstein, P., Hurtt, G., Knutti, R., Kriegler, E., Lamarque, J. F., Lowe, J., Meehl, G. A., Moss, R., Riahi, K., and Sanderson, B. M.: The Scenario Model Intercomparison Project (ScenarioMIP) for CMIP6, Geosci. Model Dev., 9, 3461–3482, https://doi.org/10.5194/gmd-9-3461-2016, 2016.

Oudar, T., Cattiaux, J., and Douville, H.: Drivers of the Northern Extratropical Eddy-Driven Jet Change in CMIP5 and CMIP6 Models, Geophys. Res. Lett., 47, https://doi.org/10.1029/2019GL086695, 2020.

Pianosi, F., Beven, K., Freer, J., Hall, J. W., Rougier, J., Stephenson, D. B., and Wagener, T.: Sensitivity analysis of environmental models: A systematic review with practical workflow, Environ. Model Softw., 79, 214–232, https://doi.org/10.1016/j.envsoft.2016.02.008, 2016.

Pinto, J. G., Fröhlich, E. L., Leckebusch, G. C., and Ulbrich, U.: Changing European storm loss potentials under modified climate conditions according to ensemble simulations of the ECHAM5/MPI-OM1 GCM, Nat. Hazards Earth Syst. Sci., 7, 165–175, https://doi.org/10.5194/nhess-7-165-2007, 2007.

Pinto, J. G., Karremann, M. K., Born, K., Della-Marta, P. M., and Klawa, M.: Loss potentials associated with European windstorms under future climate conditions, Clim. Res., 54, 1–20, https://doi.org/10.3354/cr01111, 2012.

Prahl, B. F., Rybski, D., Kropp, J. P., Burghoff, O., and Held, H.: Applying stochastic small-scale damage functions to German winter storms, Geophys. Res. Lett., 39, https://doi.org/10.1029/2012GL050961, 2012.

Priestley, M. D., Dacre, H. F., Shaffrey, L. C., Hodges, K. I., and Pinto, J. G.: The role of serial European windstorm clustering for extreme seasonal losses as determined from multi-centennial simulations of high-resolution global climate model data, Nat. Hazards Earth Syst. Sci., 18, 2991–3006, https://doi.org/10.5194/nhess-18-2991-2018, 2018.

Priestley, M. D., Ackerley, D., Catto, J. L., Hodges, K. I., McDonald, R. E., and Lee, R. W.: An Overview of the Extratropical Storm Tracks in CMIP6 Historical Simulations, J. Climate, 33, 6315–6343, https://doi.org/10.1175/JCLI-D-19-0928.1, 2020.

Priestley, M. D. K. and Catto, J. L.: Future changes in the extratropical storm tracks and cyclone intensity, wind speed, and structure, Weather Clim. Dynam., 3, 337–360, https://doi.org/10.5194/wcd-3-337-2022, 2022.

Rajczak, J., Kotlarski, S., Salzmann, N., and Schär, C.: Robust climate scenarios for sites with sparse observations: A two-step bias correction approach, Int. J. Climatol., 36, 1226–1243, https://doi.org/10.1002/joc.4417, 2016.

Ranson, M., Kousky, C., Ruth, M., Jantarasami, L., Crimmins, A., and Tarquinio, L.: Tropical and extratropical cyclone damages under climate change, Climatic Change, 127, 227–241, https://doi.org/10.1007/s10584-014-1255-4, 2014.

Röösli, T., Appenzeller, C., and Bresch, D. N.: Towards operational impact forecasting of building damage from winter windstorms in Switzerland, Meteor. Appl., 28, https://doi.org/10.1002/met.2035, 2021.

Saltelli, A.: Making best use of model evaluations to compute sensitivity indices, Comput. Phys. Commun., 145, 280–297, https://doi.org/10.1016/S0010-4655(02)00280-1, 2002.

Saltelli, A., Ratto, M., Andres, T., Campolongo, F., Cariboni, J., Gatelli, D., Saisana, M., and Tarantola, S.: Global Sensitivity Analysis. The Primer, John Wiley & Sons, Ltd, Chichester, England, Hoboken, NJ, https://doi.org/10.1002/9780470725184, 2008.

Saltelli, A., Annoni, P., Azzini, I., Campolongo, F., Ratto, M., and Tarantola, S.: Variance based sensitivity analysis of model output. Design and estimator for the total sensitivity index, Comput. Phys. Commun., 181, 259–270, https://doi.org/10.1016/j.cpc.2009.09.018, 2010.

Saltelli, A., Aleksankina, K., Becker, W., Fennell, P., Ferretti, F., Holst, N., Li, S., and Wu, Q.: Why so many published sensitivity analyses are false: A systematic review of sensitivity analysis practices, Environ. Model Softw., 114, 29–39, https://doi.org/10.1016/j.envsoft.2019.01.012, 2019.

Schwierz, C., Köllner-Heck, P., Mutter, E. Z., Bresch, D. N., Vidale, P. L., Wild, M., and Schär, C.: Modelling European winter wind storm losses in current and future climate, Climatic Change, 101, 485–514, https://doi.org/10.1007/s10584-009-9712-1, 2010.

Seiler, C. and Zwiers, F. W.: How will climate change affect explosive cyclones in the extratropics of the Northern Hemisphere?, Clim. Dyn., 46, 3633–3644, https://doi.org/10.1007/s00382-015-2791-y, 2016.

Seneviratne, S., Zhang, X., Adnan, M., Badi, W., Dereczynski, C., Di Luca, A., Ghosh, S., Iskandar, I., Kossin, J., Lewis, S., Otto, F., Pinto, I., Satoh, M., Vicente-Serrano, S., Wehner, M., and Zhou, B.: Weather and Climate Extreme Events in a Changing Climate, p. 1513–1766, Cambridge University Press, Cambridge, United Kingdom and New York, NY, USA, https://doi.org/10.1017/9781009157896.013, 2021.

Severino, L.: The Impact of Climate Change on Winter Storm Damage in Europe, Master thesis, ETH Zurich, 2022.

Shaw, T. A., Baldwin, M., Barnes, E. A., Caballero, R., Garfinkel, C. I., Hwang, Y. T., Li, C., O'Gorman, P. A., Rivière, G., Simpson, I. R., and Voigt, A.: Storm track processes and the opposing influences of climate change, Nat. Geosci., 9, 656–664, https://doi.org/10.1038/ngeo2783, 2016.

640 Sobol, I. M.: Global sensitivity indices for nonlinear mathematical models and their Monte Carlo estimates, Math. Comput. Simul., 55, 271–280, 2001.

Tebaldi, C. and Knutti, R.: The use of the multi-model ensemble in probabilistic climate projections, Philos. Trans. R. Soc. A, 365, 2053–2075, https://doi.org/10.1098/rsta.2007.2076, 2007.

645 Vautard, R., Jan Van Oldenborgh, G., Otto, F. E., Yiou, P., De Vries, H., Van Meijgaard, E., Stepek, A., Soubeyroux, J. M., Philip, S., Kew, S. F., Costella, C., Singh, R., and Tebaldi, C.: Human influence on European winter wind storms such as those of January 2018, Earth Syst. Dyn., 10, 271–286, https://doi.org/10.5194/esd-10-271-2019, 2019.

Walz, M. A. and Leckebusch, G. C.: Loss potentials based on an ensemble forecast: How likely are winter windstorm losses similar to 1990?, Atmos. Sci. Lett., 20, https://doi.org/10.1002/asl.891, 2019.

650 Welker, C., Röösli, T., and N. Bresch, D.: Comparing an insurer's perspective on building damages with modelled damages from pan-European winter windstorm event sets: A case study from Zurich, Switzerland, Nat. Hazards Earth Syst. Sci., 21, 279–299, https://doi.org/10.5194/nhess-21-279-2021, 2021.

Wilkinson, S., Dunn, S., Adams, R., Kirchner-Bossi, N., Fowler, H. J., González Otálora, S., Pritchard, D., Mendes, J., Palin, E. J., and Chan, S. C.: Consequence forecasting: A rational framework for predicting the consequences of approaching storms, Clim. Risk Manag., 35, 655 100 412, https://doi.org/10.1016/j.crm.2022.100412, 2022.

Zappa, G. and Shepherd, T. G.: Storylines of Atmospheric Circulation Change for European Regional Climate Impact Assessment, J. Climate, 30, 6561–6577, https://doi.org/10.1175/JCLI-D-16-0807.s1, 2017.

Zappa, G., Shaffrey, L. C., Hodges, K. I., Sansom, P. G., and Stephenson, D. B.: A multimodel assessment of future projections of north atlantic and european extratropical cyclones in the CMIP5 climate models, J. Climate, 26, 5846–5862, https://doi.org/10.1175/JCLI-D-660 12-00573.1, 2013.

Zumwald, M., Knüsel, B., Baumberger, C., Hirsch Hadorn, G., Bresch, D. N., and Knutti, R.: Understanding and assessing uncertainty of observational climate datasets for model evaluation using ensembles, Wiley Interdiscip. Rev. Clim. Change, 11, https://doi.org/10.1002/wcc.654, 2020.